PLA - 90 - 1

1 / 8 / 90

1 GeV リ ニ ア ッ ク 検 討 資 料

1 GeV LINAC DESIGN NOTE

題目 (TITLE) The 1 GeV Proton Linac for the Japanese Hadron Facility

著者 (AUTHOR) Y. Yamazaki et al.

概要 (ABSTRACT)

Proposed design of the 1 GeV proton linac for the Japanese Hadron Facility is described together with rationale for the design parameters. The linac is composed of a volume production type H^- ion source, a 432 MHz RFQ linac (3 MeV), a 432 MHz DTL (150 MeV) and a 1296 MHz high-β linac (1 GeV). Problems expected in each part are discussed and possible remedies are also presented.

KEY WORDS:

Ion source, RFQ, DTL, CCL, Magnet, Monitor, Beam Dynamics,
Transport, Vacuum, Cooling
Klystron, Low level rf, High power rf, Modulator
Control, Operation, Radiation, Others

高エネルギー物理学研究所 *KEK*

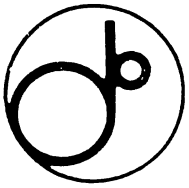

KEK Preprint 87-159
February 1988
A

THE 1 GeV PROTON LINAC FOR THE JAPANESE HADRON FACILITY

Y. Yamazaki, S. Anami, H. Baba, S. Fukumoto, T. Kageyama, T. Kato

M. Kihara, Y. Mori, A. Takagi, E. Takasaki and A. Ueno

National Laboratory for High Energy Physics

Oho, Tsukuba-shi, Ibaraki 305, Japan

S. Arai and N. Tokuda

Institute for Nuclear Study, University of Tokyo

Midori-cho, Tanashi-shi, Tokyo 188, Japan

* Invited talk given by Y. Yamazaki at the Advanced Hadron Facility Accelerator Design Workshop, Los Alamos National Laboratory, Los Alamos, U.S.A., February 22 - 27, 1988.

National Laboratory for High Energy Physics, 1988

KEK Reports are available from:

Technical Information Office
National Laboratory for High Energy Physics
1-1 Oho, Tsukuba-Shi
Ibaraki-ken, 305
JAPAN

Phone: 0298-64-1171
Telex: 3652-534 (Domestic)
(0)3652-534 (International)
Cable: KEKOHO

THE 1 GeV PROTON LINAC FOR THE JAPANESE HADRON FACILITY

Y. Yamazaki, S. Anami, H. Baba, S. Fukumoto, T. Kageyama, T. Kato
M. Kihara, Y. Mori, A. Takagi, E. Takasaki and A. Ueno

National Laboratory for High Energy Physics
Oho, Tsukuba-shi, Ibaraki 305, Japan

S. Arai and N. Tokuda

Institute for Nuclear Study, University of Tokyo
Midori-cho, Tanashi-shi, Tokyo 188, Japan

Abstract

Proposed design of the 1 GeV proton linac for the Japanese Hadron Facility is described together with rationale for the design parameters. The linac is composed of a volume production type H^- ion source, a 432 MHz RFQ linac (3 MeV), a 432 MHz DTL (150 MeV) and a 1296 MHz high-β linac (1 GeV). Problems expected in each part are discussed and possible remedies are also presented.

1. Introduction

A 1-GeV proton linac will be constructed to inject proton beams to various ring accelerators of the Japanese Hadron Facility.[1] Parameters of the beams to be delivered by the linac are listed in Table I. The linac has three distinctive features: 1) high energy, 2) a high average current and 3) a high duty factor of an rf system, that should be carefully taken into account in designing the linac. Also, it is required that the linac can be operated in extreme stability.

Table I Design parameters of the H^- linac

Energy	1 GeV
Total length	$\sim$ 500 m
Peak current	20 mA
Repetition rate	50 Hz
Pulse length	400 μs
Average current	$\gtrsim$ 200 μA

A high energy proton linac accelerating an intense beam with a limited length immediately requires very high rf power. Necessary rf power is further increased for the following reason. In the high intensity and high energy proton linac no beam loss is allowed at the high energy region of the accelerator, since radioactivity caused by the beam loss becomes a serious problem in a long term operation. Then, sufficiently large beam acceptances are required for all of

accelerator tanks. This requirement tends to increase bore radii of the accelerator tanks and shift synchronous phases further from the phase of the highest rf field, resulting in lower acceleration efficiency. Thus, the requirement of no beam loss also implies increase of the rf power.

It is advantageous to reduce a number of rf sources by increasing an rf power of each rf source for the purposes of stable operation, easy maintenance and cost performance. Development of the high power rf sources requires a high power modulator. Thus, our effort was mainly devoted to development of the high power modulator.

A fundamental scheme of the proton linac was proposed as shown in Fig. 1. The linac will be composed of an ion source, an RFQ linac, a drift-tube linac (DTL) and a high-ß linac. Negative hydrogen beams will be accelerated, since its injection efficiency is higher than the multi-turn injection of proton beams.

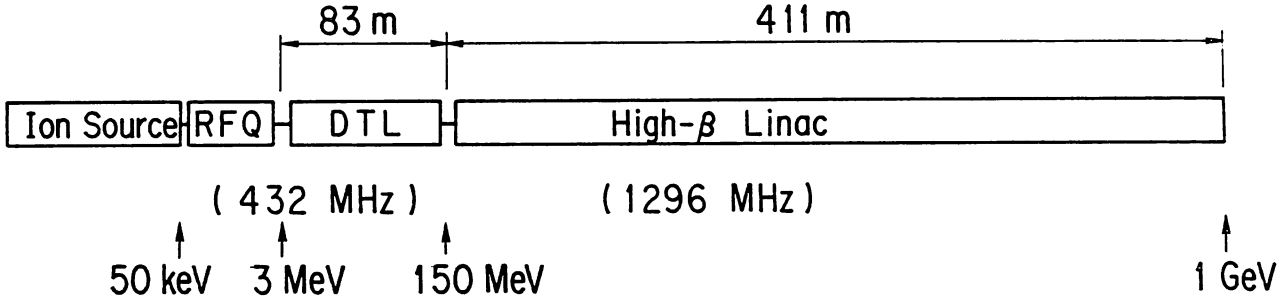

Fig. 1 The scheme of the proton linac.

Among various parameters of linacs, an accelerating frequency is one of the most important parameters, since cost and performance of the linacs will be strongly dependent upon the frequency. In general both of shunt impedances and possible accelerating fields of cavities with the same figure increase proportionally to a square root of the resonant frequency. However, as the frequency increases, sizes of accelerating cavities and klystrons decrease, so that cooling of these RF parts becomes difficult and beam acceptances of the cavities decrease. Thus, the nearly highest frequency should be chosen, so far as the cooling of the RF parts is feasible and the beam acceptance is large enough. Also, it is advantageous to choose the frequency, at which commercial klystrons are available. Taking these factors into account, we have chosen 1296 MHz for the frequency of the high-ß linac and 432 MHz for those of the RF quadrupole and drift-tube linac.

2. Ion Source

We are planning to use a volume production type H^- ion source rather than a surface plasma type multi-cusp ion source whose possible cesium vapor flow will reduce the breakdown voltage of the following RFQ. We have developed a test model of the ion source, whose typical parameters are listed in Table II.

Table II Typical parameters of the test H^- ion source of the volume-production type

Arc current	140 A
Arc voltage	150 V
Filament current	75 A × 4
Hydrogen gas flow	5 sccm
Anode bias	+ 5 V
Acceleration voltage	30 kV

Attempt was made to optimize parameters of a magnetic filter. Since low energy electrons ($\lesssim$ 1 eV) that play an important role in production of H^- ions are selectively extracted from a chamber filled with plasma through the magnetic filter, the beam current of the H^- ions is strongly dependent upon a field strength, a field direction, and a position of the magnetic filter. The obtained field dependence of the beam current is shown in Table III. Further optimization of the parameters is in progress.

Table III Dependence of the beam current on the field strength of the magnetic filter integrated along the extraction system

Integrated magnetic field (Gauss·cm)	Beam current density (mA/cm^2)
650	0.3
455	0.6
245	1.5

An extraction system of the ion source should be carefully designed to satisfy conflicting requirements: high extraction efficiency of the H^- ion beam and low electron beam loading. Our preliminary result was not yet satisfactory. For example, the electrons of more than 50 mA/cm^2 flowed into the first extraction electrode in the last case of the Table III. It was found that the electron beam loading was largely affected by the field strength and position of the magnetic filter. Therefore, the problem of the electron beam loading should be also taken into account in optimizing the parameters of the magnetic filter.

In order to increase the beam current density we are planning to investigate its dependence on the volume of the ion source. It is expected that the density of the excited hydrogen molecules would be increased by decreasing the volume of the ion source at the same arc condition, resulting in increase of the H^- beam current. Also, our future plan includes the measurement of beam emittances.

3. RFQ Linac

The H^- beam from the ion source will be injected to a 432 MHz four-vane type RFQ linac at the injection energy of 50 keV and will be accelerated to 3 MeV. Design parameters of the RFQ linac are listed in

Table IV. Phase-space projections at the first cell are shown in Fig. 2 together with those at the last cell. Matching of the emitted beams from the ion source to the acceptance of the RFQ will be made by a magnetic lens installed between the ion source and RFQ.

Table IV Parameters of the 432 MHz H^- RFQ (four-vane)

Frequency (f)	432 MHz
Input energy (T_{in})	0.05 MeV
Output energy (T_{out})	3 MeV
Vane length	269 cm
Number of cells	305
Mean bore radius (r_0)	0.340 cm
Minimum bore radius (a_{min})	0.236 cm
Margin of bore radius (a_{min}/a_{max})	1.25
Maximum modulation (m_{max})	1.83
Cavity diameter (D)	15.4 cm
Normalized acceptance (A_n) (100%)	1.5 π mm·mrad
(90%)	1.0
Normalized emittance at 3 MeV (100%)	2.6
(90%)	1.3
Kilpatrick factor (f_k)	1.8
(Maximum surface field ($E_{s,max}$)	361 kV/cm)
Intervane voltage (V)	90 kV
Focusing strength (B)	4.0
Maximum defocusing strength (Δ_b)	-0.078
Cavity wall loss (P_c)	980 kW[a]
Transmission (0 mA)	98 %
(20 mA)	94 %

a It is assumed that the quality factor is 60 percent of the calculated value.

The parameters were determined to obtain a normalized acceptance of 1.5 π mm·mrad for the beam current of 20 mA with the maximum electric field $E_{s,max}$ of 1.8 times of the Kilpatrick limit. Then, the minimum bore radius becomes 0.236 cm with the vane length of 269 cm. The total wall loss amounts to about 1 MW.

The RFQ linac with the small bore radius will require rigid tolerance limits on dimensional errors, and it is difficult to machine, assemble and align the long vanes accurately. Also, it will be hard to cool the vanes with this dimension for the wall loss of 1 MW. To test a feasibility of the RFQ linac with these parameters a prototype RFQ linac is going to be fabricated.

Modification of the parameters of the RFQ linac to make manufacturing of the RFQ easier, for example, by reduction of the accelerating energy and/or frequency, may require change of parameters of the following drift-tube linac. Thus, possibility of the modification will be discussed in the next section.

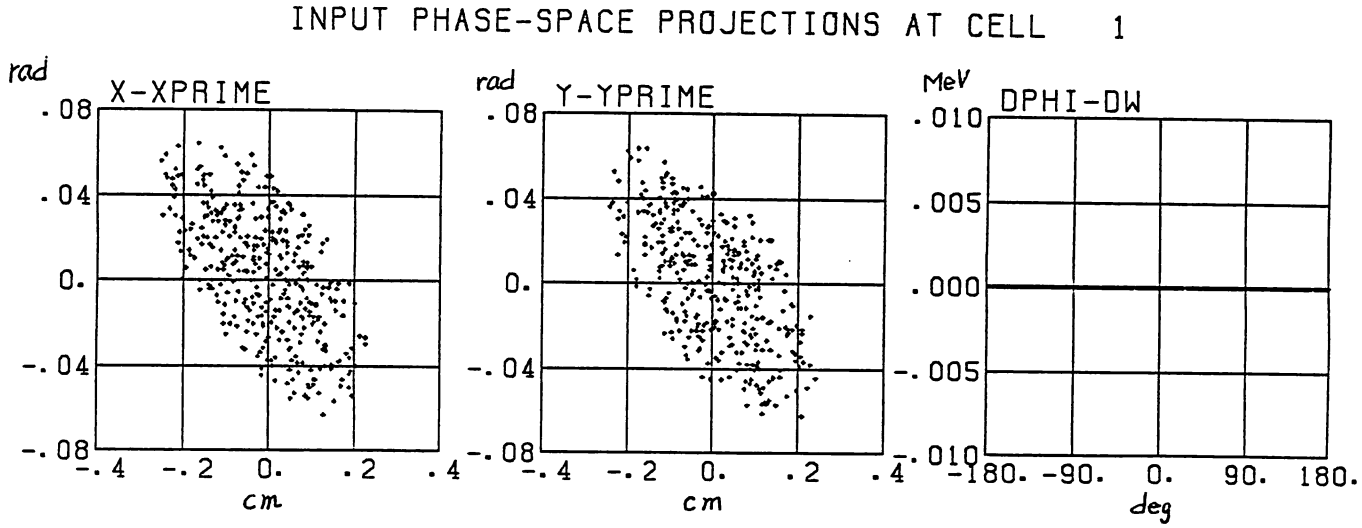

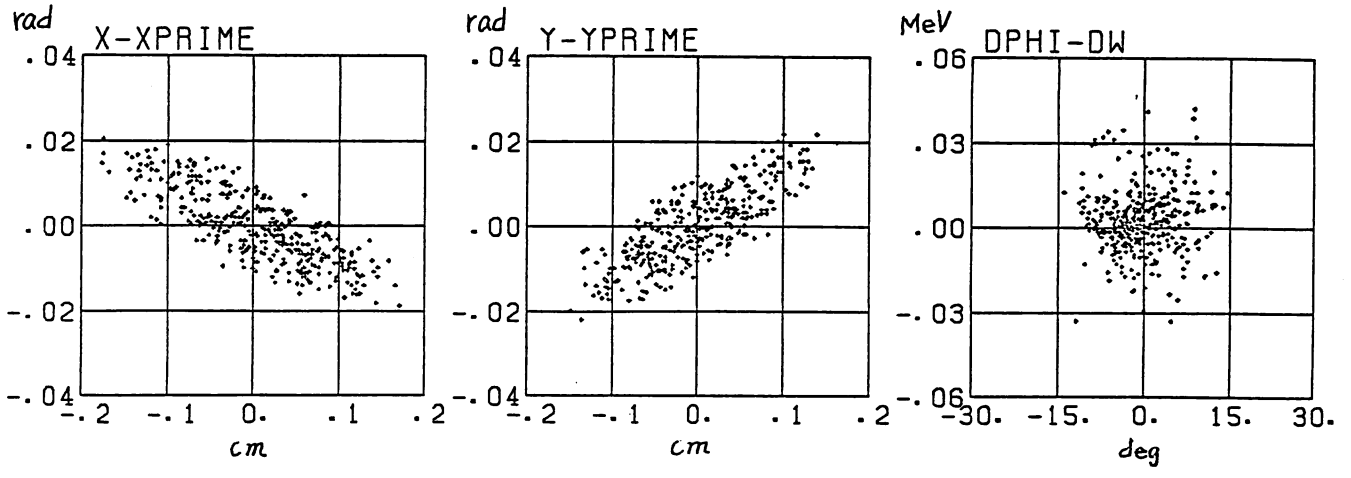

Fig. 2 Phase-space projections at the first and last cells of the 432 MHz RFQ linac.

4. Drift-tube Linac.

A 432 MHz drift-tube linac (DTL) will accelerate the beam from 3 MeV to 150 MeV. A choice of the output energy will be discussed in the next section in relation with a high-ß linac. Parameters of the drift-tube linac are listed in Table V. The linac will be separated into 13 tanks, each of which will be driven by a 1 MW klystron. Shunt impedances of the drift-tube linac are shown in Fig. 3 as a function of ß = v/c. It is noted that the drift-tube linac consists of four types of tanks. Three parameters of an inner diameter of tanks, an outer diameter and a corner radius of drift-tubes were approximately optimized to obtain the highest shunt impedances for each type of tanks, keeping the maximum surface electric field within 75 per cent of the Kilpatrick limit.

Table V Parameters of the drift-tube linac and high-ß linac

	DTL	High-ß linac
Frequency (f)	432 MHz	1296 MHz
Input energy (T_{in})	3 MeV	148 MeV
Output energy (T_{out})	148 MeV	1017 MeV
Acceleration field (E_0)	3 MV/m	3.6 ∿ 4.4 MV/m[a]
Synchronous phase (ϕ_s)	-26°[b]	-30°[c]
Tank length	75.7 m	303.0 m[d]
Total length	83.3 m	410.9 m
Bore radius	0.5 cm	1.5 cm
Number of cells	342	3568
Number of tanks	13	152
Total wall loss (P_c)	9.0 MW[e]	81.7 MW[f]
Beam loading (P_b)[g]	2.9 MW	17.4 MW
Total power (P_g)	11.9 MW	99.1 MW
Number of klystrons[h]	13	36
Klystron power	1.0 MW	3.0 MW
Normalized acceptance[i]		
$A_{x,n}$ (90 %)	8.9 π mm·mrad	29 π mm·mrad
$A_{x,n}$ (100 %)	10.0 π mm·mrad	36 π mm·mrad
$A_{y,n}$ (90 %)	8.8 π mm·mrad	26 π mm·mrad
$A_{y,n}$ (100 %)	10.0 π mm·mrad	34 π mm·mrad
Acceptable		
Input energy spread (ΔW_{in})	0.30 MeV	3.0 MeV
Output energy spread (ΔW_{out})	1.44 MeV	8.8 MeV
Acceptable		
Input phase spread ($\Delta\phi_{in}$)	88°	87°
Output phase spread ($\Delta\phi_{out}$)	24°	32°

a. Acceleration fields are increased as ß increases to make an input power per tank approximately equal.

b. Except for the first tank. A synchronous phase of the first tank is 30°.

c. Synchronous phase at the first cell of each tank. Lengths of cells of a tank are made equal, resulting in the maximum phase slip of -27°.

d. Includes space for quadrupole magnets, steering magnets and beam monitors.

e. 1.3 times of the calculated value.

f. 1.2 times of the calculated value.

g. For the beam current of 20 mA.

h. Possible power losses at wave guides and circulators are not included.

i. Constant field gradients of B' = 200 T/m and B' = 23.2 T/m are used for the DTL and high-ß linac, respectively, with an FD lattice.

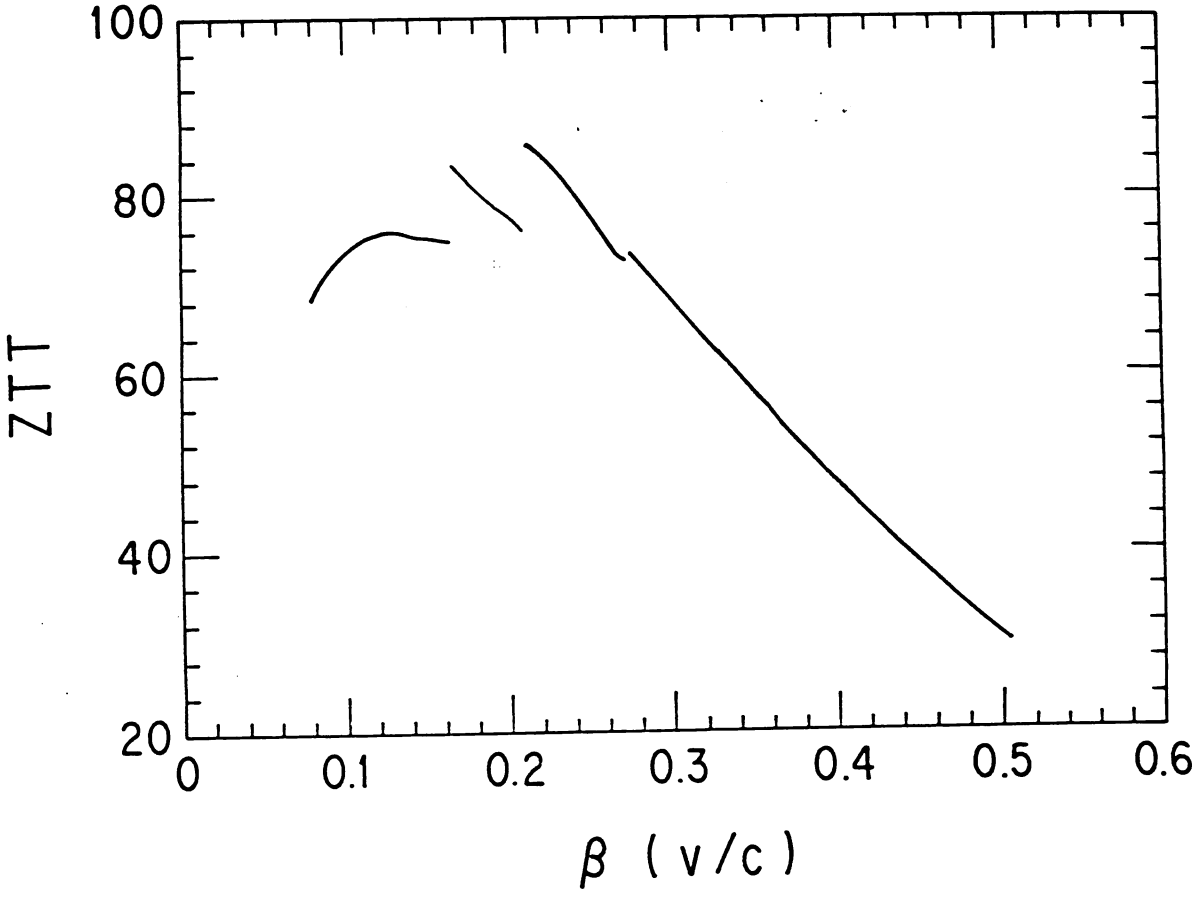

Fig. 3 Shunt impedances of the drift-tube linac as a function of ß. The values in MΩ/m as calculated with the SUPERFISH are plotted.

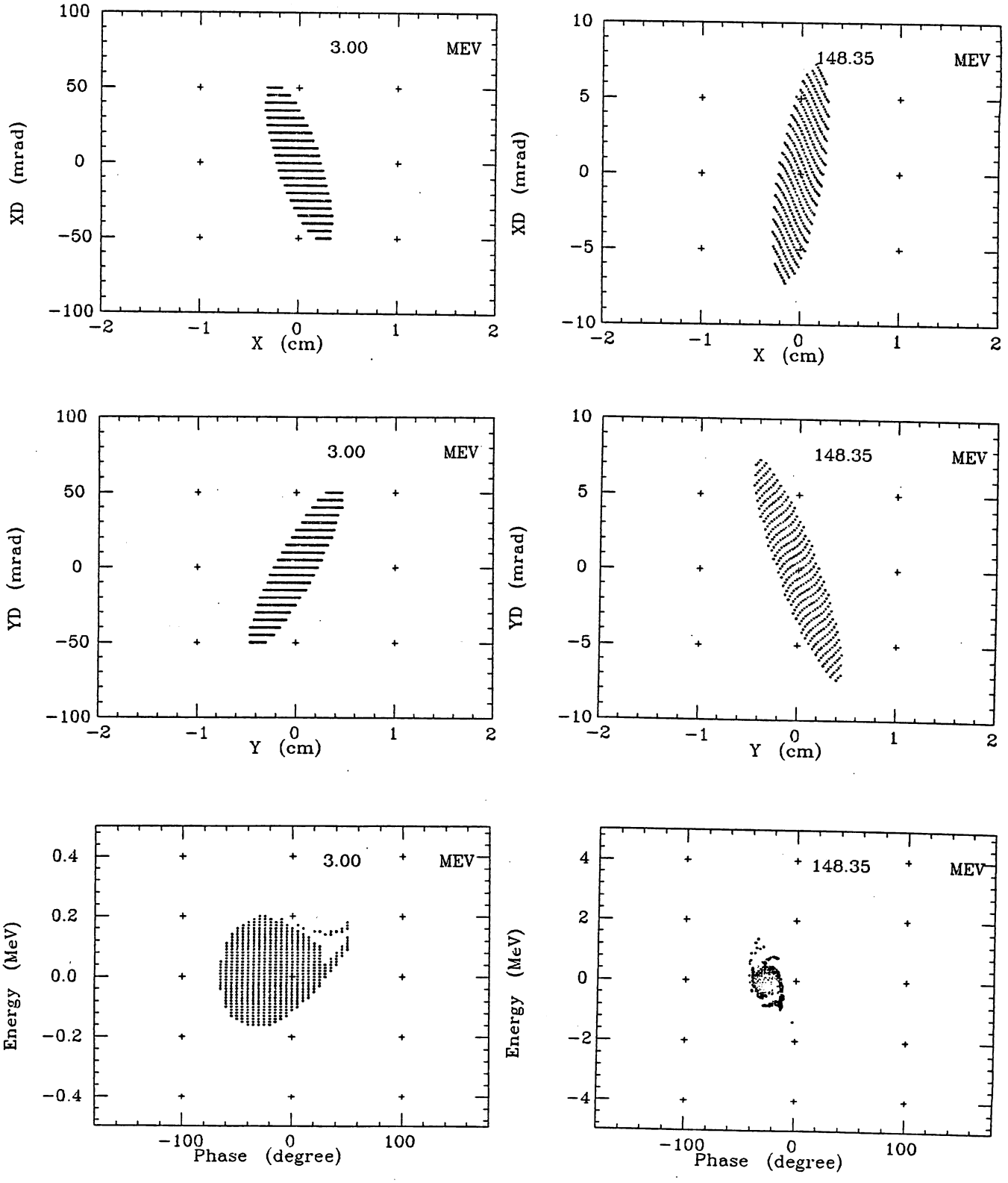

Fig. 4 Phase-space projections at the edges of the first and last quadrupole magnets of the DTL.

Longitudinal and transverse acceptances of the drift-tube linac are shown in Fig. 4 and Table V, together with the emittances of the accepted beams at 150 MeV. Here, an FD lattice is used with constant quadrupole magnetic field gradient of B' = 200 T/m.

It is seen that the transverse acceptances of the DTL are by a factor of about 3 larger than the emittances of the RFQ. A matching section will be necessary between the end of the vanes of the RFQ and the first quadrupole magnet of the DTL. Otherwise, adjustable electromagnets will be required for the first several cells, although permanent magnets are to be used for the other cells.

The 88° phase acceptance of the DTL will be large enough for the 30° phase emittance of the RFQ even with the drift space between the RFQ and DTL. Even if the frequency of the RFQ is halved to increase the bore radius of the RFQ, the DTL can longitudinally accept the beams from the RFQ. Therefore, it is worthwhile to investigate the possibility of the 216 MHz RFQ linac, although another type of a 216 MHz RF power source is required in this case.

We are planning to use permanent magnets made of SmCo, since the permanent magnets require neither of wiring nor water-cooling for the magnets, that is, become maintenance-free and SmCo can produce a strong magnetic field, being rather stable against effects due to radiation. However, it is difficult to seal the drift tubes containing the SmCo, since the SmCo cannot stand the high temperature used for the silver brazing and the strong magnetic field produced by the SmCo inhibits conventional use of the electron-beam welding (EBW). At present attempts to seal the drift-tubes containing the SmCo are in progress by a few methods including EBW and laser welding, but results are not yet satisfactory. It will be another method to expose the SmCo to vacuum, and outgassing measurement of the SmCo in vacuum is in progress.

If we accelerate the 2 MeV beam with the DTL to shorten the length of the RFQ, lengths of drift tubes for 2 MeV to 3 MeV become too short to contain the permanent SmCo with necessary focusing strengths. Then, it is inevitable to use electromagnets for the low energy region. Probably, this is more difficult choice for the 432 MHz DTL than the development of the 3 MeV RFQ linac.

5. High-ß Linac

Standing wave linacs are more advantageous than traveling wave linacs, if RF pulse widths are longer than filling times ($\sim$ a few μs typically). The $\pi/2$ mode operation of a multi-cell cavity is necessary to keep a high degree of stability of the accelerating field against effects due to heavy beam loading and manufacturing imperfections. Then, possible candidates for the high-ß cavity structure are alternating periodic structure (APS) without nose cones or coupling slots, alternating periodic structure with nose cones and coupling slots, side-coupled structure (SCS), disc-and-washer structure (DAW) and annular-coupled structure (ACS).

For the annular-coupled structure it was reported that serious depression of a quality factor is arising from excitation of a coupling-cell quadrupole mode.[2] Although a possible remedy was proposed,[2] extensive study will be necessary to solve the problem. In the disc-and-washer structure a TM1 passband crosses the accelerating frequency. A method to keep the TM1 passband away from the accelerating frequency decreases a shunt impedance seriously.[3]

Both of the alternating periodic structure and side-coupled structure are free from these troubles. However, in the alternating periodic structure coupling cells are located on the beam axis, consuming space for accelerating cells, and space for the coupling cells is relatively limited compared with the side-coupling structure. Therefore, a shunt impedance of the alternating periodic structure is lower than that of the side-coupled structure, and a quality factor of the coupling mode of the APS is lower than that of the SCS resulting in more strict requirement for manufacturing accuracy.[4] On the other hand the axially symmetric structure of the APS, in particular, without coupling slots has the following advantages. The field of the TM0 mode of the APS is more symmetric. Machining and assembling of the APS are easier, allowing a more variety of assembling methods. Also, we have lots of experience in manufacturing and operation of the APS that is used in the TRISTAN rings. Therefore, we decided to develop both of the side-coupled structure and alternating periodic structure in parallel for the time being. In the following paragraphs, however, results of computation with the SCS are presented as an example.

Shunt impedances of the SCS calculated with a computer program SUPERFISH are shown in Fig. 5 as a function of ß. A rather large bore radius of 1.5 cm as 1296 MHz structure was chosen to obtain a large transverse acceptance. The gap length was adjusted to optimize the shunt impedance.

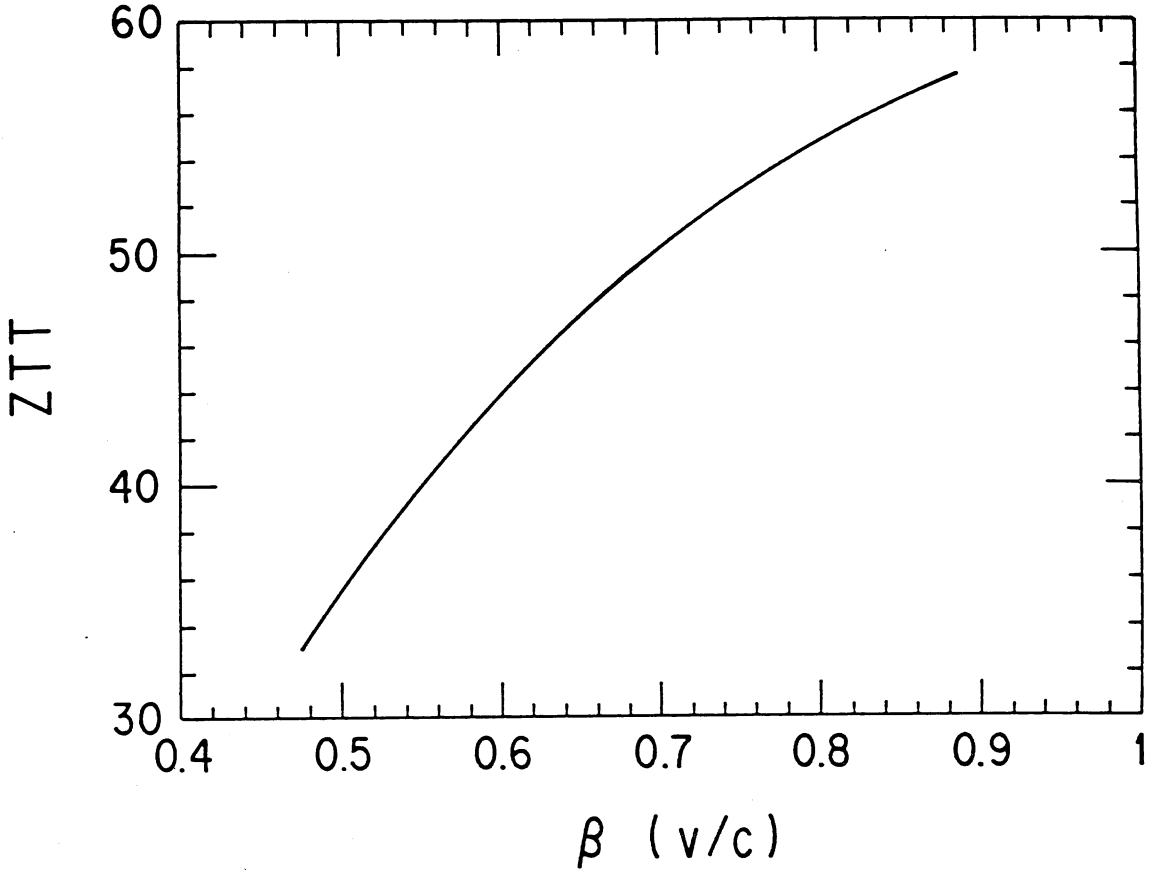

Fig. 5 Shunt impedances of the side-coupled linac as a function of ß. The values in MΩ/m as calculated with the SUPERFISH are plotted.

The sizes of the coupling slot was determined to obtain a coupling constant of 5 percent with a three dimensional computer program MAFIA.[5] With this coupling constant the quality factor of the accelerating mode was reduced by 7 percent. Assuming rather large decrease of 13 percent of the quality factor, for example, due to cavity wall imperfections, we estimated necessary RF power as shown in Table V. The high-ß linac will be driven by 36 klystrons with 3 MW.

A proposed typical configuration of the high-ß accelerating tanks is shown in Fig. 6. The drift space between two tanks have space enough for two quadrupole magnets and either of a steering magnet or a beam monitor. Shorter tanks will be used in the low energy side to increase transverse acceptances. Transverse and longitudinal acceptances thus obtained are shown in Table V and Fig. 7 together with emittances of the output beams.

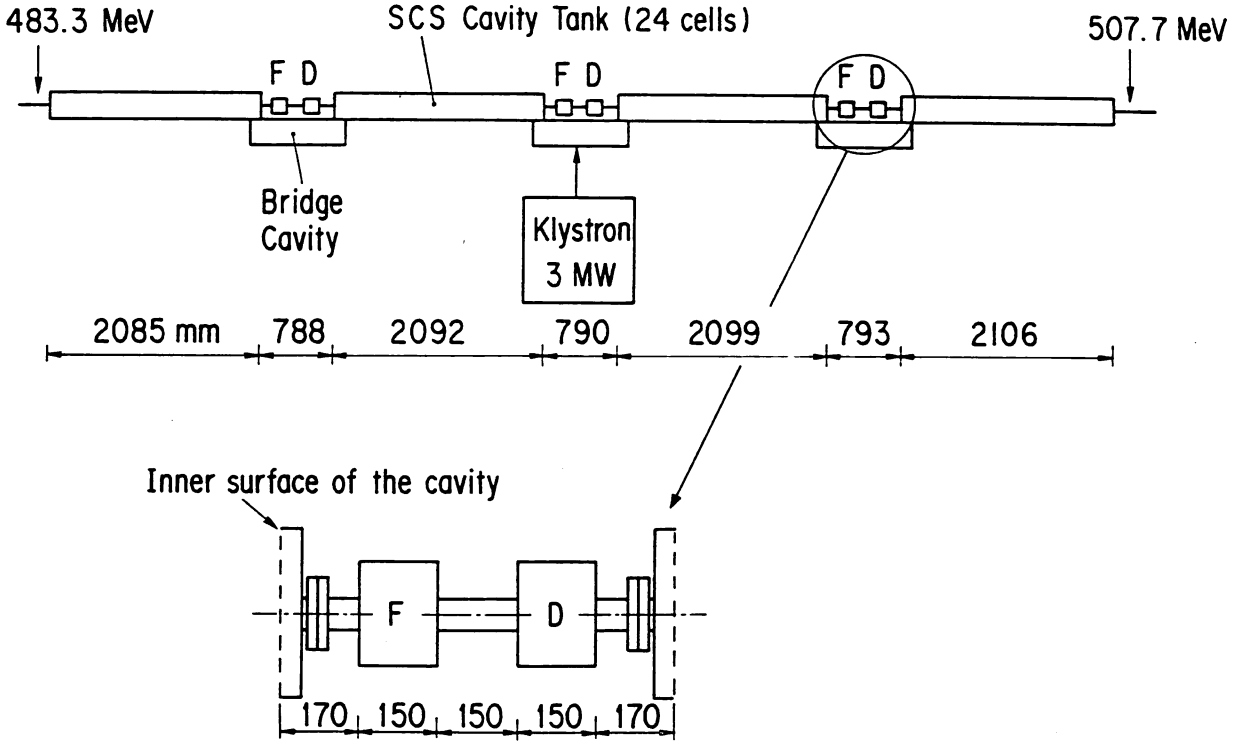

Fig. 6 A typical configuration of the high-ß linac.

It is seen that the normalized transverse acceptances of the high-ß linac is about 3 times of those of the DTL and 10 ∿ 15 times of those of the RFQ. However, it should be noted that the acceptances were computed only for the synchronous beams. Dependence of the transverse acceptances on the phase of the injected beam is shown in Fig. 8. It is seen that the transverse acceptances will be reduced to 60 percent

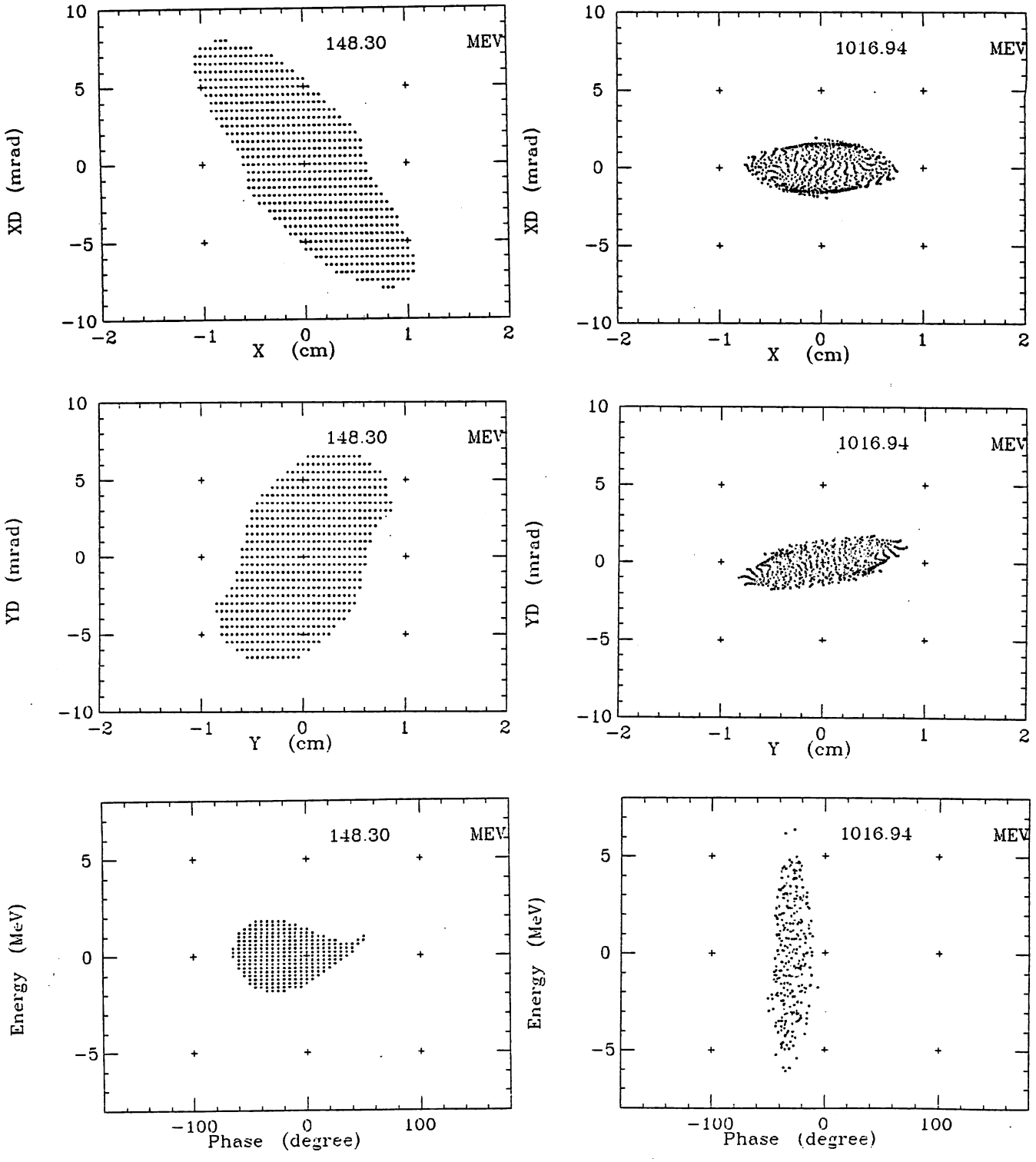

Fig. 7 Phase-space projections at the first and last cells of the high-ß linac.

of those of the synchronous beams, if the beam phase is located near the separatrix. Thus, more detailed study will be necessary, including study of effects due to possible imperfect alignment of the cavities and quadrupole magnets, to decrease the bore radius of the cavities.

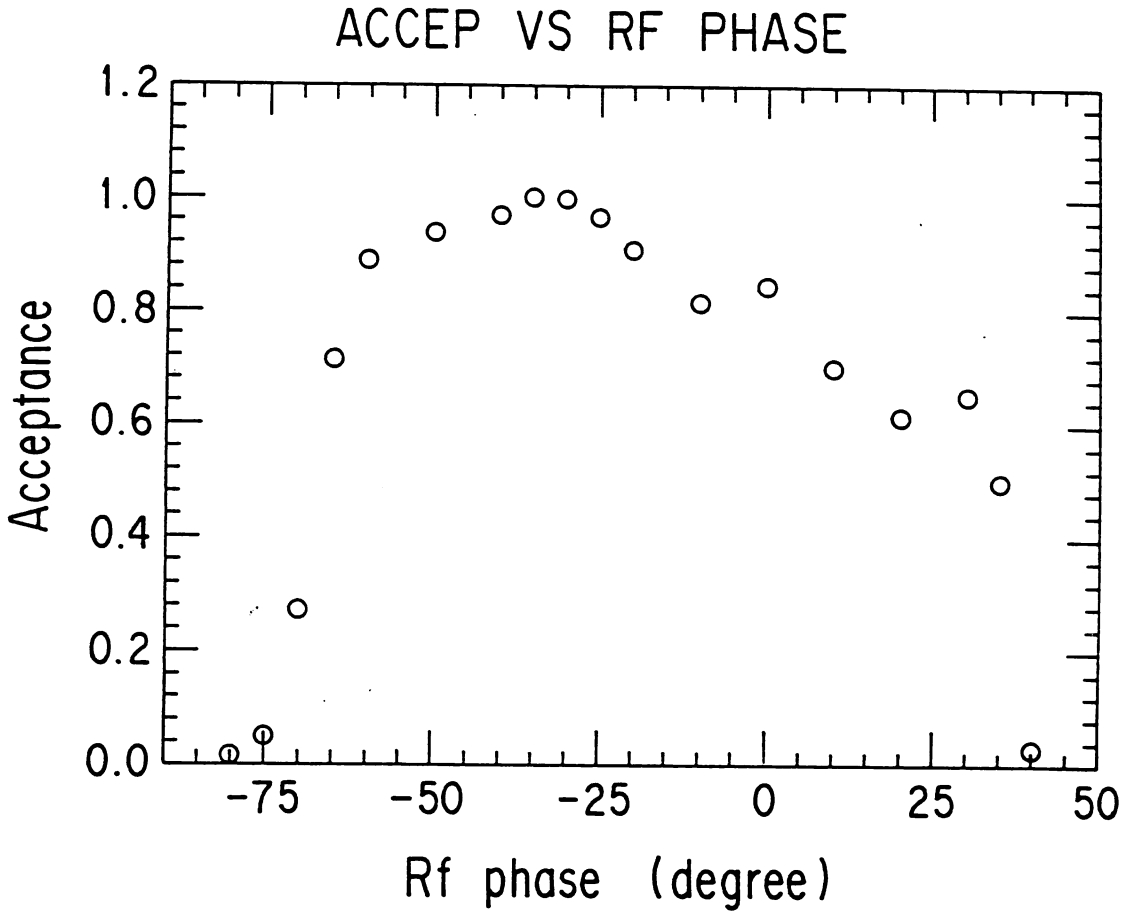

Fig. 8 Dependence of the transverse acceptances on the phase of the injected beam. The values relative to that for the synchronous beam are plotted.

The phase acceptance of the high-ß linac is only slightly larger than the phase emittance of the DTL, since the frequency of the high-ß linac is 3 times of the DTL. However, it will yield no serious problem, since debunching in a drift space between the DTL and high-ß linac will be small.

Comparing the shunt impedances of the high-ß linac with those of the DTL, one may propose that a transition energy from the DTL to the high-ß linac should be lowered to save the RF power. This modification is also advantageous in cost of the linac, since the DTL is generally more expensive than the high-ß linac. However, if the gap length approaches to the bore diameter as ß decreases, it was found that the shunt impedances of the SCS and APS began to drop drastically. Therefore, to lower the transition energy one must decrease the bore radius simultaneously. This modification will increase the shunt impedances

further and, thus, is very attractive. For this modification, however, extensive study is necessary for various effects that may deteriorate the beam acceptance.

For detailed design of the high-ß linac including tuning method and so on it is required to estimate machining and assembling errors and to find the best method of welding or brazing. Thus, attempt is being made to fabricate the cavities using silver-brazing, electron-beam welding, electroplating welding and diffusion welding.

6. Modulator

One of the most difficult parts of the proposed 1-GeV proton linac will be a high power modulator that drives the 3 MW klystron with a long pulse (600 μs) and a high duty factor (3 %). Also, it should be operated with extreme stability and reliability. Therefore, our effort has been mainly devoted to development of the high power modulator. We decided to develop a line-type modulator rather than the other types, for example, a hard-tube modulator for the following reasons. First, we have some experience for line-type modulators. Second, line-type modulators provide stable pulses with relatively simple circuits whose behaviors can be easily understood. Third, efficiencies of line-type modulators are better than hard-tube pulsers. Finally, running costs will be less expensive, since no replacement of the tubes is necessary. Power-grid tubes used in hard-tube modulators are very large and expensive, while their life time cannot be expected to be long.

The line-type modulator is composed of a HV dc power supply with an IVR, a charging unit with a de-Qing circuit, a pulse forming network (PFN) and a discharging unit as shown in Fig. 9. Its output pulse voltage is stepped up to 7 times by a pulse transformer.

We have designed a prototype modulator for a 6 MW klystron rather than the 3 MW klystron for the following reason. In order to obtain klystrons that can be stably operated at 3 MW in unsaturated region, it is necessary to develop klystrons with the power capability of 5 or 6 MW. Development of the 6 MW klystrons requires a modulator with an output power of 15 MW for a klystron efficiency of 40 %, and successful development of the modulator will directly lead to development of stable modulators for 3 MW klystrons at the same time. Parameters of the modulator designed for the 6 MW klystrons are listed in Table VI. It is noted that a cabinet for the PFN and discharging circuit becomes very big: 9 m wide, 1.7 m deep and 2.7 m high, because of a very long pulse width.

Taking account of its high duty factor and long pulse length we designed each part of the modulator as follows. Since averaged power is very high compared with usual modulators, for example, for electron linacs, averaged power loss in capacitors and inductors of the PFN will be very large. Thus, a capacitor of each PFN section is divided into four parts to obtain efficient heat radiation by increasing their surfaces. Also, for the inductor of each PFN section made of a coil and an iron core whose inductance is variable, the core laminated by very thin iron sheets (0.1 mm thick) is used to reduce an eddy current loss in the core. A cross section of the iron core is made relatively large to prevent it from saturation even for the case of a shorted load. Otherwise, if a load of the modulator happens to be shorted, for example, by a possible discharge or spark in a klystron, extraordinarily high voltage will be produced between terminals of the inductor result-

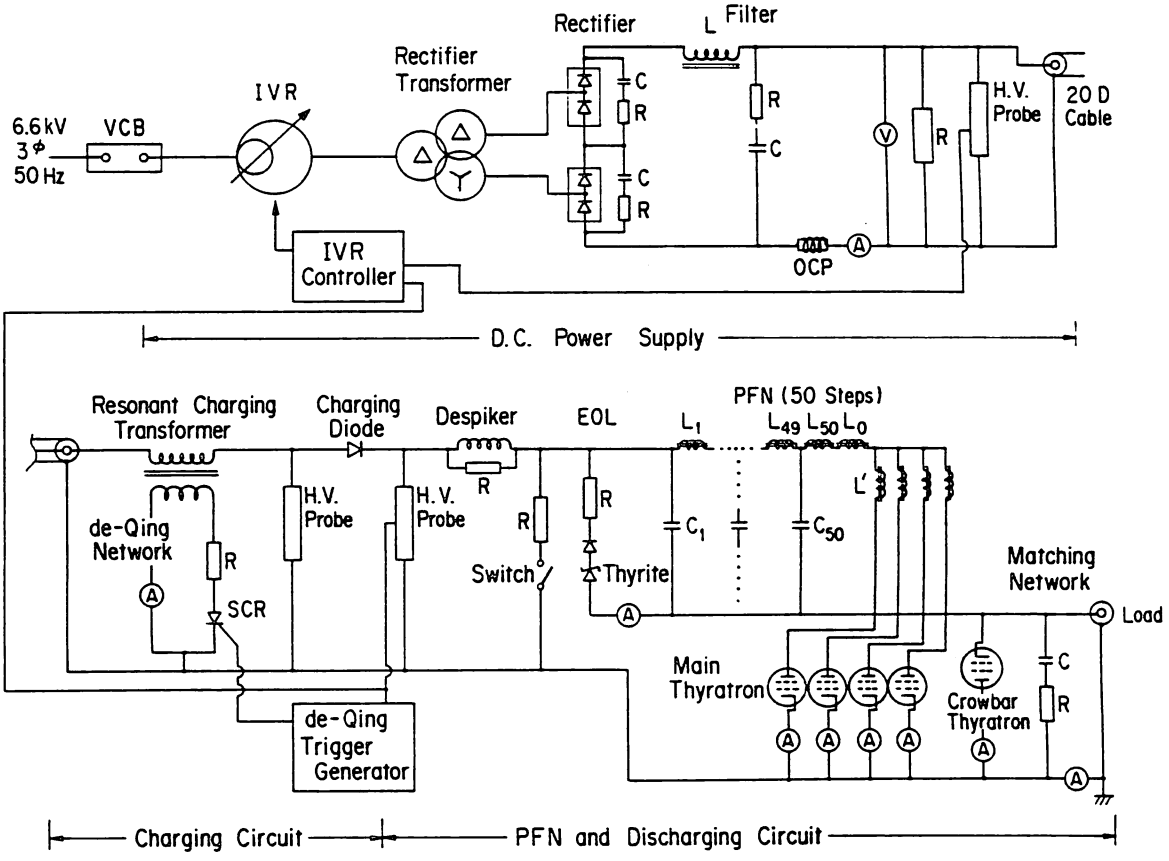

Fig. 9 The test line-type modulator.

Table VI Parameters of the test modulator for a 6 MW klystron

Peak power	15 MW
Average power	450 KW
Output voltage	20 kV
Output current	750 A
PFN impedance	26.7 Ω
Load impedance	26.7 Ω
Pule width (half value)	600 μs
(flat top)	520 μs
Pulse rise time	< 30 μs
Flatness	< 0.5 %
Repetition rate	50 pps
Pulse voltage stability	
(short term)	< 0.2 %
(long term)	< 0.5 %/h

ing in break-down of the inductor.

Another effect of the high averaged power is that an available switching thyratron cannot stand the high averaged current. Thus, four thyratrons are used in parallel operation as a switching element. Differences among rise times of the thyratrons are corrected by equipping their anodes with variable inductors. Differences among the averaged currents of the thyratrons will be made uniform by adjusting the hydrogen gas pressure in the thyratron tubes.

The high duty factor and long pulse width imply that a ratio of a kick-out time (pulse length) from the PFN to a charging time is not negligibly small. During the kick-out time the charging current through the thyratrons builds up to a considerable value. This phenomenon gives rise to difficulty in turning-off of the switching thyratrons. Thus, when the output pulse is falling, an output circuit will be shorted by firing a crowbar thyratron to produce a reflected inverse voltage pulse, whose negative pulse will forcibly turn off the switching tube.

Finally, an inductance of the pulse transformer becomes very large because of the long pulse width. It is almost comparable to that of the charging choke transformer. Then, it becomes difficult to stabilize a charging voltage for the PFN by a de-Qing method, since energy stored in the pulse transformer remains. Thus, a shunt circuit composed of diodes and resistors must be connected to primary winding terminals of the pulse transformer.

References

1) M. Kihara, KEK Preprint 86-106 and references therein.
2) R. K. Cooper et al., Preprint LA-UR-83-95.
3) S. Inagaki, Nucl. Instr. Meth. A251, 417 (1986).
4) Y. Yamazaki, T. Higo and K. Takata, Part. Accel. in print.
5) T. Weiland, Part. Accel. 17, 227 (1985).